Journal of Nematology 33(4):227–238. 2001.

Ultrastructure and Development of *Pasteuria* sp. (S-1 strain), an Obligate Endoparasite of *Belonolaimus longicaudatus* (Nemata: Tylenchida)

R. M. Giblin-Davis,[1] D. S. Williams,[2] W. P. Wergin,[3] D. W. Dickson,[4] T. E. Hewlett,[4] S. Bekal,[5] and J. O. Becker[5]

Abstract: Pasteuria sp., strain S-1, is a gram-positive, obligate endoparasitic bacterium that uses the phytoparasitic sting nematode, *Belonolaimus longicaudatus,* as its host in Florida. The host attachment of S-1 appears to be specific to the genus *Belonolaimus* with development occurring only in juveniles and adults of *B. longicaudatus.* This bacterium is characterized from other described species of *Pasteuria* using ultrastructure of the mature endospore. Penetration, development, and sporogenesis were elucidated with TEM, LTSEM, and SEM and are similar to other nematode-specific *Pasteuria.* Recent analysis of 16S rDNA sequence homology confirms its congeneric ranking with other *Pasteuria* species and strains from nematodes and cladocerans, and corroborates ultrastructural, morphological, morphometric, and host-range evidence suggesting separate species status.

Key words: Belonolaimus longicaudatus, development, obligate nematode endoparasitic bacterium, *Pasteuria* sp. (S-1 strain), sporogenesis, sting nematode, ultrastructure.

Investigators have identified four nominal species of *Pasteuria* that are gram-positive, mycelial, endospore-forming, and endoparasitic on nematodes and crustaceans. The type species, *Pasteuria ramosa,* parasitizes water fleas (Cladocera; Daphinidae) (Ebert et al., 1996; Metchnikoff, 1888; Sayre et al., 1979, 1983), while the other three species are reported in association with phytoparasitic nematodes. *Pasteuria penetrans* parasitizes root-knot nematodes, *Meloidogyne* spp. (Mankau, 1975; Sayre and Starr, 1985; Starr and Sayre, 1988); *P. thornei* parasitizes root-lesion nematodes, *Pratylenchus* spp. (Starr and Sayre, 1988; Sayre et al., 1988); and *P. nishizawae* parasitizes the cyst nematodes, *Heterodera* and *Globodera* (Sayre et al., 1991b). *Pasteuria* strains are globally distributed and have been reported attached to and parasitizing numerous nematode species (>300) from different trophic groups including plant-parasitic, predatory, insect-parasitic, and free-living nematodes (Atibalentja et al., 2000; Cianco et al., 1994). The biology and taxonomy of *Pasteuria* have been obscure and difficult to study because of their small size and highly host-specific and obligate endoparasitic nature (Chen and Dickson, 1998; Dickson et al., 1994; Ebert et al., 1996; Giblin-Davis, 2000; Giblin-Davis et al., 1990). Monoxenic culture attempts have been unsuccessful due to a lack of knowledge about these fastidious bacteria and the physiology of their nematode hosts (Bishop and Ellar, 1991; Riese et al., 1988; Williams et al., 1989). Thus, traditional procedures for biochemical characterization have not been available for elucidation of *Pasteuria* species (Sayre and Starr, 1985). The four nominal species of *Pasteuria* were described using a Linnean species concept that relied upon morphometrics, ultrastructural comparisons of mature endospores, and host attachment trials. Cianco (1995) challenged the reliability of morphometrics and host range for *Pasteuria* taxonomy. Numerous potential *Pasteuria* species, which exist in soil and freshwater habitats, may overlap considerably in morphometrics and host range (Chen and Dickson, 1998). Ultrastructure of mature endospores appears to provide reliable traits in the few species of *Pasteuria* that have been named, especially when used in combination with morphometrics and host range (Ebert et al., 1996; Sayre et al., 1991a, 1991b; Sayre and Starr, 1985; Starr and Sayre, 1988). However, this still leaves a dearth of taxonomic characters with phylogenetic value. Recent phylogenetic analyses of 16S rDNA sequences from *P. ramosa* (U34688; Ebert et al., 1996), *P. penetrans* (AF077672; Anderson et al., 1999; Bekal et al., 2001), *Pasteuria* sp. ex *Heterodera glycines* (AF1 34868; Atibalentja et al., 2000), and *Pasteuria* sp., strain S-1 ex *Belonolaimus longicaudatus* (AF254387; Bekal et al., 2001) have generated hypotheses about the placement of the genus *Pasteuria* within the bacterial kingdom, with relationship to the genus *Alicyclobacillus* (Atibalentja et al., 2000; Ebert et al., 1996) and provided independent evidence concerning species relationships that can be used with ultrastructural and host specificity data.

We examined the development and ultrastructure of the mature endospore of a putative new species of *Pasteuria* (S-1 strain) from the sting nematode, *B. longicaudatus* from Florida, previously referred to as an isolate of the *Pasteuria penetrans* group, *Pasteuria* sp., or *Pasteuria* n. sp. (S-1) (Bekal et al., 1999, 2001; Dickson et al., 1994; Giblin-Davis, 1990, 2000; Giblin-Davis et al., 1990, 1995).

Materials and Methods

Sources of S-1 Pasteuria: Belonolaimus longicaudatus were collected from soil around the roots of bermudagrass

Received for publication 05 February 2001.

[1] University of Florida-IFAS, Fort Lauderdale Research and Education Center, 3205 College Ave., Davie, FL 33314-7799.

[2] Microbiology and Cell Science, University of Florida, PO Box 110700, Gainesville, FL 32611-0700.

[3] Nematology Laboratory, USDA, ARS, Bldg. 011-A, BARC-West, Beltsville, MD 20705.

[4] Department of Entomology and Nematology, University of Florida-IFAS, PO Box 110620, Gainesville, FL 32611-0620.

[5] Department of Nematology, University of California, Riverside, CA 92521. E-mail: giblin@ufl.edu

The authors thank Henry Aldrich, Janete Brito, Barbara J. Center, Z. X. Chen, Billy Crow, and James F. Preston for help, discussions, and ideas used in this project and Monica Elliott and Nigel Harrison for review of the manuscript. This research was supported by a grant from the United States Golf Association. This manuscript is Florida Agricultural Experiment Stations Journal Series R-07848.

This paper was edited by Patricia Timper.

(*Cynodon* spp.) grown in plots at the Fort Lauderdale Research and Education Center, Davie, Florida (26°05′ 12″N 080°14′ 26″W). The nematodes were separated from the soil using the sugar-flotation-centrifugation method (Jenkins, 1964). The S-1 strain had previously been collected from this site (Bekal et al., 1999, 2001; Giblin-Davis, 2000; Giblin-Davis et al., 1990, 1995). Live nematodes were examined using an Olympus BH-2 photomicroscope fitted with Nomarski optics and a camera lucida to identify the stage of nematode, attachment of endospores to the cuticle, and presence of different stages of internal parasitism. Crystal violet staining (<1%; w/v) was used to increase visibility of externally attached spores. Endospore measurements were made from samples of spores from five different nematodes collected from this site. Counts of mature endospores from spore-filled cadavers were done by collecting different stages of *B. longicaudatus* that were filled with spores, squashing them individually in a drop of water, then counting the spores in a set volume on a hemocytometer. In addition, *B. longicaudatus* with apparent endospore infestations of S-1 from soil around bermudagrass roots on a golf course in Orlando, Florida, and from soil around potato plants in Hastings, Florida, were collected and processed for transmission electron microscopic (TEM) comparisons with the Davie, Florida isolate.

Conventional and low-temperature scanning electron microscopy of S-1 Pasteuria: We examined the external morphology of S-1 from Davie, Florida, with conventional scanning electron microscopy (SEM) and low-temperature scanning electron microscopy (LTSEM). For SEM, specimens of *B. longicaudatus* with attached spores were fixed in 3% (v/v) glutaraldehyde, dehydrated in a graded ethanol series, critical point dried from liquid CO_2, mounted on a stub with double sticky tape, sputtercoated with 20 nm of gold-palladium, and viewed with a Hitachi (Tokyo, Japan) S-4000 Field Emission SEM at 7 kV. For LTSEM, live *B. longicaudatus* with attached spores were placed onto tissue paper and mounted onto a stub. In addition, live *B. longicaudatus* with internal infestations of sporulating S-1 were collected in deionized water and placed into 24-K gold, hinged-holders mounted on a Denton complimentary freeze-etch specimen cap (Wergin et al., 1993). Specimens were cryofixed by submersion in an Oxford (Oxford, UK) nitrogen slush chamber. The chamber was evacuated, and the cap was withdrawn into the cryotransfer arm and transferred to the Oxford prechamber, where a pre-cooled pick was used to fracture samples in the complimentary caps by lifting and rotating the fracture arm 180° (Wergin et al., 1993). Specimens were then sputter-coated with platinum in the pre-chamber and inserted onto the cryostage of the microscope for observation on a Hitachi S-4100 field emission scanning electron microscope equipped with an Oxford CT- 1500 Cryotrans System at 10 kV.

Transmission electron microscopy of S-1 Pasteuria: S-1-infected specimens of *B. longicaudatus* for study of mature endospore ultrastructure or changes during penetration, development, and sporogenesis were cut into two or more pieces and fixed in 2% (v/v) glutaraldehyde, 2% (v/v) formaldehyde, in 0.1 M sodium cacodylate buffer (pH 7.2) overnight at 4 °C, embedded in 2 to 3% (w/v) agarose, and cut into small blocks. The glutaraldehyde was rinsed from the blocks with five rinses of 0.1 M sodium cacodylate buffer, and the tissue was postfixed in 2% (w/v) OsO_4 in 0.1 M sodium cacodylate buffer and 1% (w/v) aqueous uranyl acetate. The tissue was dehydrated in an ethanol-acetone series, and embedded in Spurr's epoxy resin. Thin-sections were cut with a diamond knife on an LKB Ultratome III or an RMC MT-6000-XL ultramicrotome, stained with uranyl acetate and lead citrate, and viewed with a Hitachi H-7000 or a Zeiss-EM10 (Thornwood, NY) TEM.

Results and Discussion

The ultrastructure of the mature endospore of S-1 is distinctive when compared with endospores of the named species of *Pasteuria* (Giblin-Davis, 2000; Giblin-Davis et al., 1990, 1995). The terminology used herein to describe endospore morphology was previously defined by Sturhan et al. (1994). With SEM and LTSEM, peripheral fibers of the mature endospore unevenly protrude around the exposed spherical outer coat of the spore creating a crenate border (Fig. 1B–D) that is similar to that observed for a *Pasteuria* strain from *Hoplolaimus galeatus* from Peru (Cianco et al., 1998). The exosporium and sporangium can be retained upon spore attachment to the host cuticle (Fig. 1B) or be lost, exposing the microfibrillar surface coat on the dorsum of the peripheral fibers (Fig. 1D), similar to *P. penetrans* (Chen et al., 1997; Sayre and Starr, 1985) and *P. nishizawae* (Sayre et al., 1991a, 1991b).

TEM observations of mature endospores of S-1 inside the host (Figs. 2, 3) and attached to the cuticle of a host (Fig. 4) revealed very little morphological variability. S-1 and S-1-like strains from *B. longicaudatus* from different geographical regions and host plants in Florida were not different (Fig. 2) but were distinct from all other described species of *Pasteuria* (Fig. 5). Some variability was observed in the size of the electron translucent area between the peripheral fibers and the central body from all samples (extremes are illustrated in Fig. 2A, B). In lateral sections, the shape of the central body of S-1 is rounded-rectangle to rounded-trapezoid (Figs. 2, 4, 5) contrasting with a circular shape for *P. ramosa* (Ebert et al., 1996), horizontally oriented elliptical shapes for *P. penetrans* (Sayre and Starr, 1985; Sayre et al., 1988) and *P. nishizawae* (Sayre et al., 1991a, 1991b), and a rounded-square shape for *P. thornei* (Starr and Sayre, 1988) (Fig. 5). The rounded-trapezoidal appearance of S-1 is partly due to the outer spore coat, which

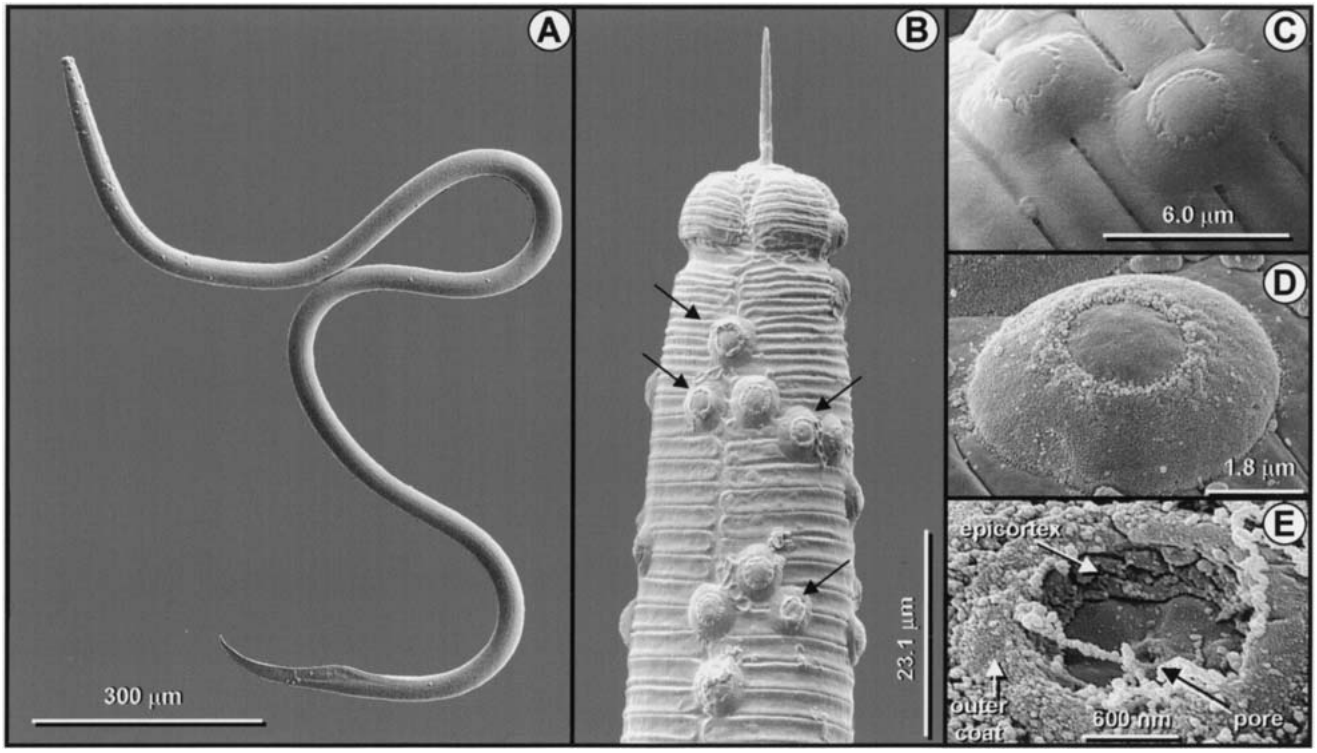

FIG. 1. Low-temperature (LTSEM) and conventional scanning electron microscopic (SEM) photomicrographs of *Pasteuria* sp. (S-1 strain) attached to *Belonolaimus longicaudatus* from Davie, FL. A) LTSEM of male *B. longicaudatus* that is encumbered with >30 spores of S-1 (note that most spores are located on head and tail ends). B) LTSEM close-up of spore-encumbered head region of *B. longicaudatus* with feeding stylet protracted. Arrows indicate spores that appear to have retained what looks like the exosporium. C) LTSEM close-up of attached S-1 spores without exosporium revealing crenate border around the exposed outer spore coat. D) SEM close-up of attached S-1 spore without exosporium and showing microfibrillar surface coating on dorsal peripheral fibers. E) SEM close-up of spent S-1 spore where top of outer spore coat has become dislodged.

is thickest laterally, thinner on top, and thinnest across the bottom of the spore, being 7 to 8 times thicker laterally than along the bottom (Figs. 2, 4, 5). This variation contrasts with the other described species, which have outer spore coats with relatively uniform thickness (Fig. 5). The thickness of the outer spore coat wall of S-1 is, at its thickest point, >15% (both walls >30%) of the diameter of the central body as compared with 3 to <13% (both walls 6 to <25%) for the other described species of *Pasteuria* (Fig. 5). This species-specific lateral thickening of the outer spore coat in S-1 is due to densely packed fibrous micro-projections that are equal in electron density to the concentric and lamellar layers of outer spore coat surrounding the inner spore coat. The projections are directed outward toward the peripheral fibers and are usually oriented perpendicular to the inner region of the outer spore coat. The micro-projections represent >30% of the total outer spore coat thickness in S-1 (Figs. 2, 3A, 4, 5) and are present in TEM micrographs of the outer spore coats of *P. penetrans* (Chen et al., 1997; Sayre et al., 1988), and *P. nishizawae* (Sayre et al., 1991a, 1991b) but represent <25% of the outer spore coat thickness (Fig. 5). They are also present in several undescribed species of *Pasteuria* (Giblin-Davis et al., 1990; Sturhan et al., 1994).

The LTSEM images of sheared spores of S-1 (Fig. 3B, C) reveal a solid central protoplast surrounded by a lattice-like cortex, enclosed in an impervious-looking inner spore coat. In other spore-forming bacteria, such as *Bacillus subtilis,* acid-soluble spore proteins (ASSPs) constitute about 5% of the total spore protein and are confined to spore protoplasm, which is synthesized during sporulation and degraded during germination (Johnson and Tipper, 1981). The outer spore coat appears as a dense lattice surrounding the inner spore coat, which is enveloped by a zone with a less dense lattice and then surrounded by a dense lattice representing the peripheral fibers. The spore is enclosed in a sheet-like exosporium that appears to be perforated with small openings allowing movement of a granular-like material. The sporangium walls of S-1 appear sheet-like with a few perforations (Fig. 3B, C).

In TEM, the epicortical wall remnant of the mature endospore of S-1 surrounds the cortex in a sublateral band (Figs. 2, 4, 5), similar to *P. thornei* but different from the other three described species (Fig. 5) (Giblin-Davis et al., 1990, 1995). The epicortical wall remnant in S-1 expands the core at the base, accentuating the trapezoidal appearance of the central body (Figs. 2, 4, 5). The epicortical wall remnant in the other described species are as follows: completely concentric in *P. ra-*

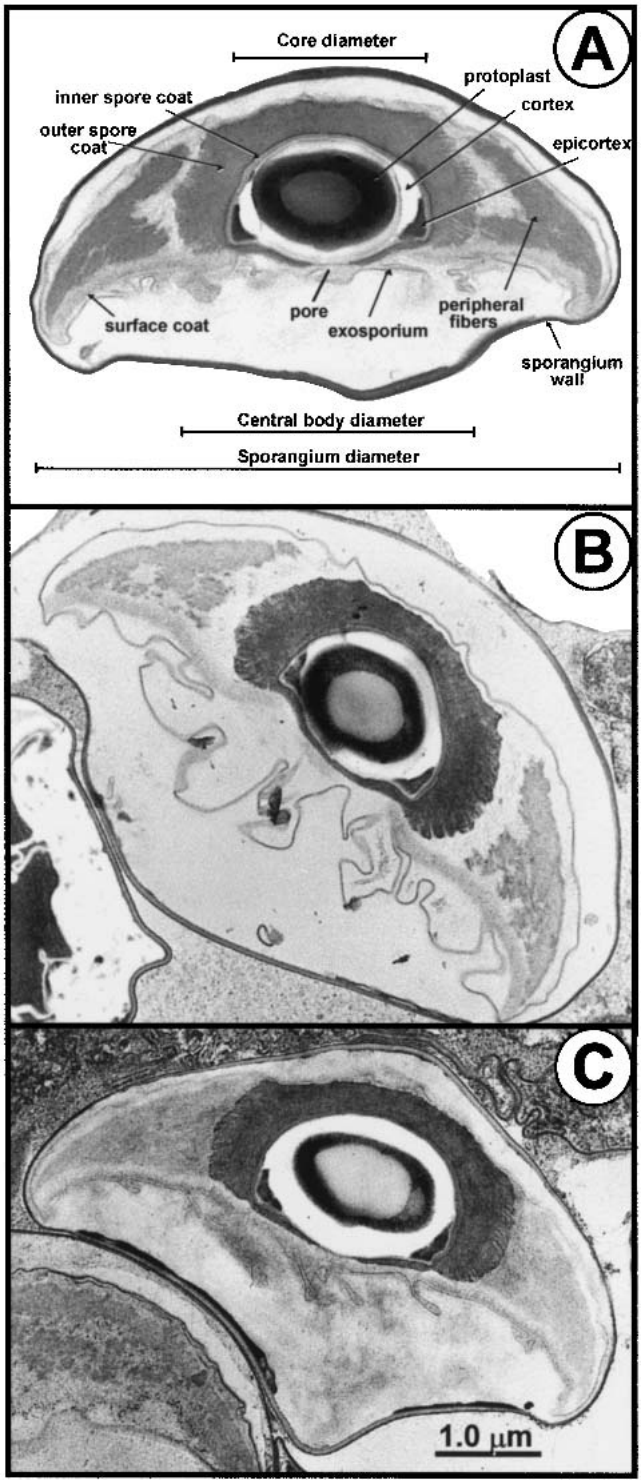

FIG. 2. Transmission electron microscopic (TEM) photomicrographs of mature endospores of *Pasteuria* sp. (S-1 strain) within *Belonolaimus longicaudatus* from different host plants and geographical locations. A) Bermudagrass host from Fort Lauderdale Research and Education Center, Davie, FL. B) Bermudagrass host from Orlando, FL. C Potato host from Hastings, FL.

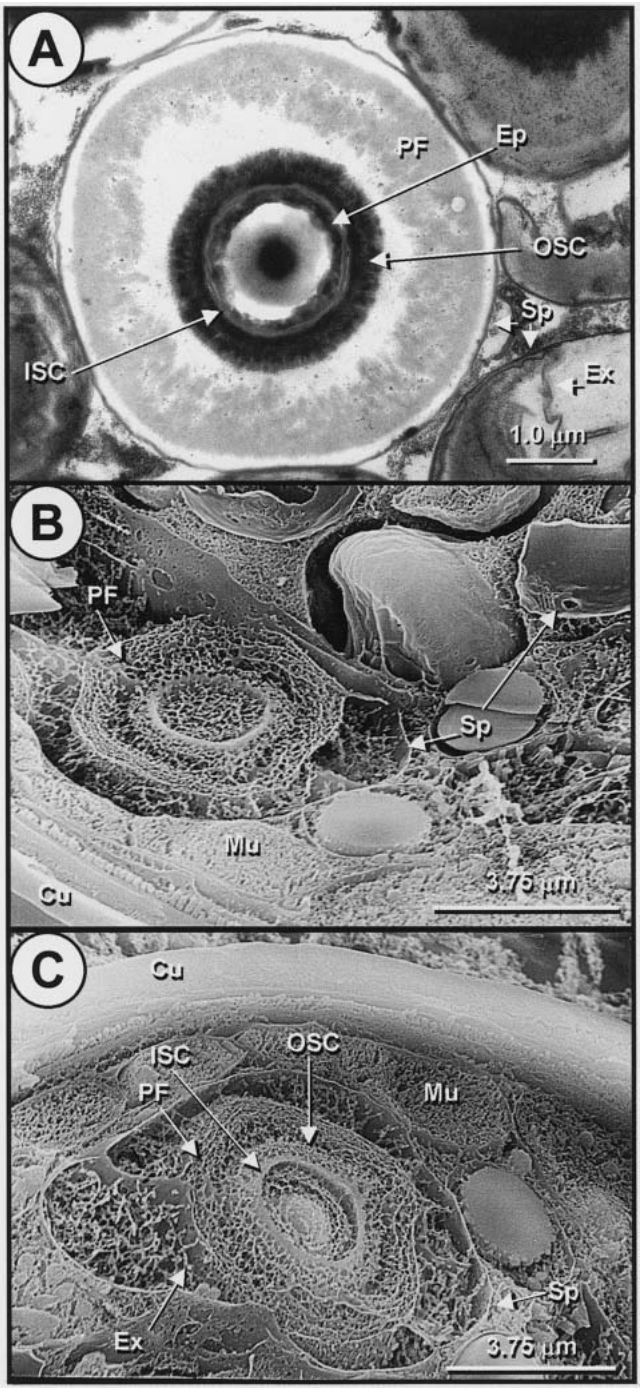

FIG. 3. Polar-oriented transverse sections of maturing endospores of *Pasteuria* sp. (S-1 strain) in *Belonolaimus longicaudatus* hosts from Davie, FL. A) TEM micrograph taken at level of the epicortical wall remnant. B) LTSEM view of a fractured section through *B. longicaudatus* exposing sectioned spore above protoplasm (other endospores visible). C) Opposing (complementary face) half of fractured nematode and spore (Cu = nematode cuticle; Ep = epicortical wall remnant; Ex = exosporium; ISC = inner spore coat; Mu = nematode somatic longitudinal muscle; OSC = outer spore coat; PF = peripheral fibers; Sp = sporangium wall).

mosa and *P. nishizawae*, and lateral in *P. penetrans* (Fig. 5) (Sayre et al., 1991b). Sayre et al. (1991b) present a drawing depicting the epicortical wall remnant of *P. ramosa* (ex *Moina rectirostris*) but then state in the text that it does not occur. However, examination of TEM micrographs in Sayre et al. (1983) and Ebert et al. (1996) suggests that an epicortical wall does exist in *P.*

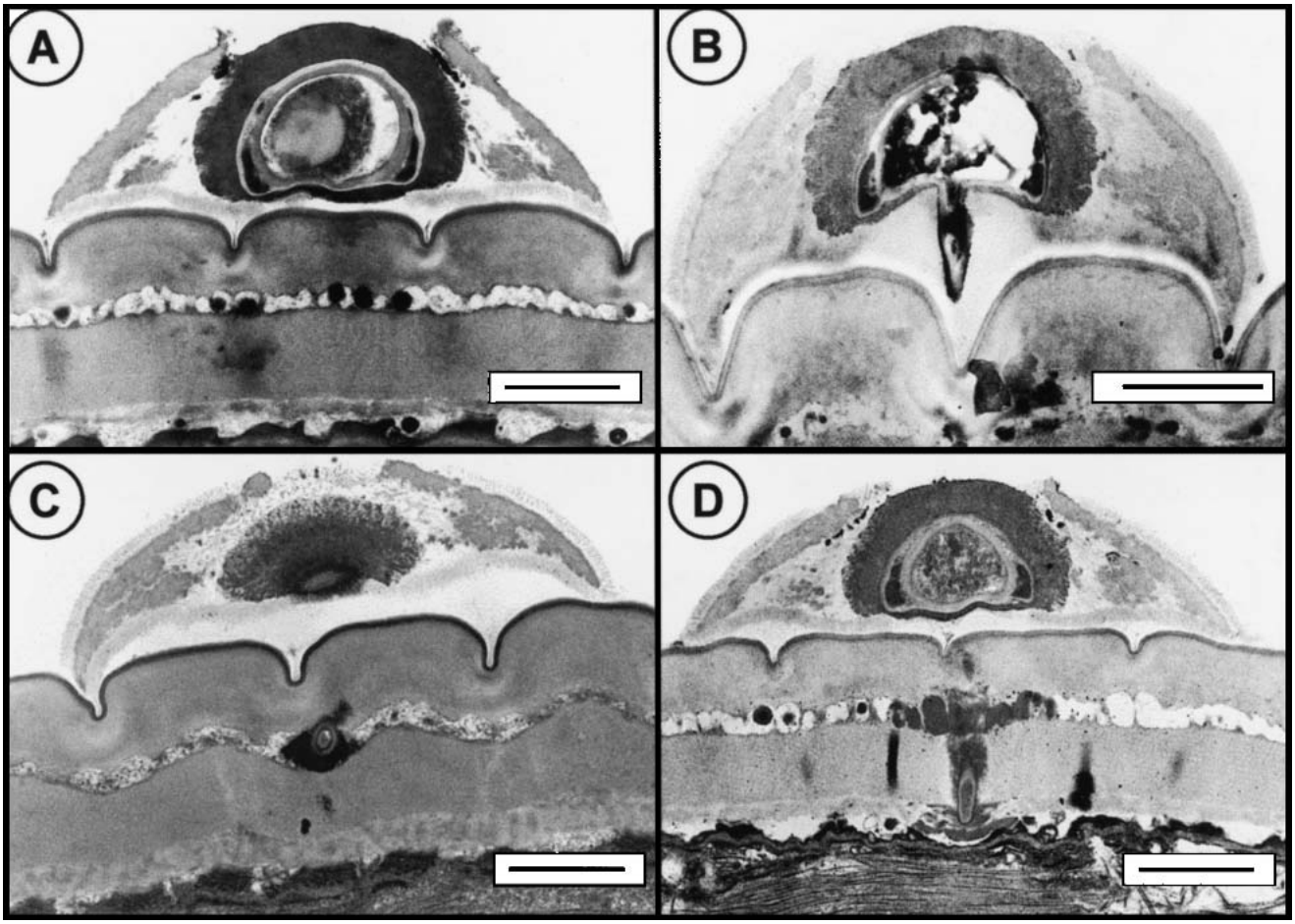

FIG. 4. TEM photomicrographs of *Pasteuria* sp. (S-1 strain) endospores that have attached, germinated, and penetrated the host cuticle of *Belonolaimus longicaudatus*. A) Attached spore. B) Attached spore with penetration tube. C) Attached and germinated spore with penetration tube running parallel to cuticular surface in the median zone of the cuticle. D) Attached and germinating spore with penetration tube penetrating through the cuticle into the epidermis but not directly under spore pore. Bar = 1.0 μm.

ramosa (ex *Moina rectirostris* and *Daphnia magna,* respectively) at stage IV of sporogenesis, prior to outer spore coat formation, and that this wall probably differentiates into three concentric layers (from the outside to the inside), outer spore coat, inner spore coat, and epicortical wall remnant in mature endospores (Fig. 5). This structure requires reexamination with more attention to ontogeny of the spore coat layers.

The pore of S-1 occurs at the ventral midpoint of the core and is about 0.3 μm in diameter (Figs. 1E, 2A), which is similar to *P. penetrans* but larger than *P. thornei* (0.1 μm) and *P. nishizawae* (0.2 μm) (Fig. 5) (Sayre et al., 1991b). No species-specific basal ring (ventral extension of the outer spore coat) occurs in S-1 around the pore opening as in *P. penetrans* (Fig. 5) (Chen et al., 1997; Sayre et al., 1988). *Pasteuria ramosa* differs from all nematode-specific *Pasteuria* in not possessing a pore or an exosporium (Ebert et al., 1996; Sayre et al., 1991b). This difference may be due in part to the mode of parasitism, which is presumed to be after ingestion and probably does not involve external attachment and penetration of the host as do the nematode-specific *Pasteuria*. Spores of nematode-specific *Pasteuria* have been observed with and without an exosporium and (or) sporangium attached to the cuticle of their hosts. However, TEM observations of attached spores have not revealed the presence of the exosporium or sporangium between the surface coat on the ventral surface of the peripheral fibers and the cuticle of the host (Fig. 4A-D) (Sayre and Starr, 1985; Sayre et al., 1988; Sturhan et al., 1994). Chen et al. (1997) showed SEM evidence of the exosporium and the sporangium being sloughed off of the dorsal surface of attached spores of *P. penetrans*. However, this observation does not explain why the exosporium is not visible between the spore and the host cuticle unless it is digested or lost at some stage. Attachment is presumed to involve the microfibrillar surface coat that resides on, or is an extension of, the peripheral fibers (part of perisporium) (Sturhan et al., 1994) of the nematode-specific *Pasteuria,* including S-1 (Figs. 2, 4). Spore attachment of *P. penetrans* is hypothesized to be mediated via glycopeptide ligand receptors (spore adhesins) in the microfibrillary layer of the spore coat that recognize and attach to correspond-

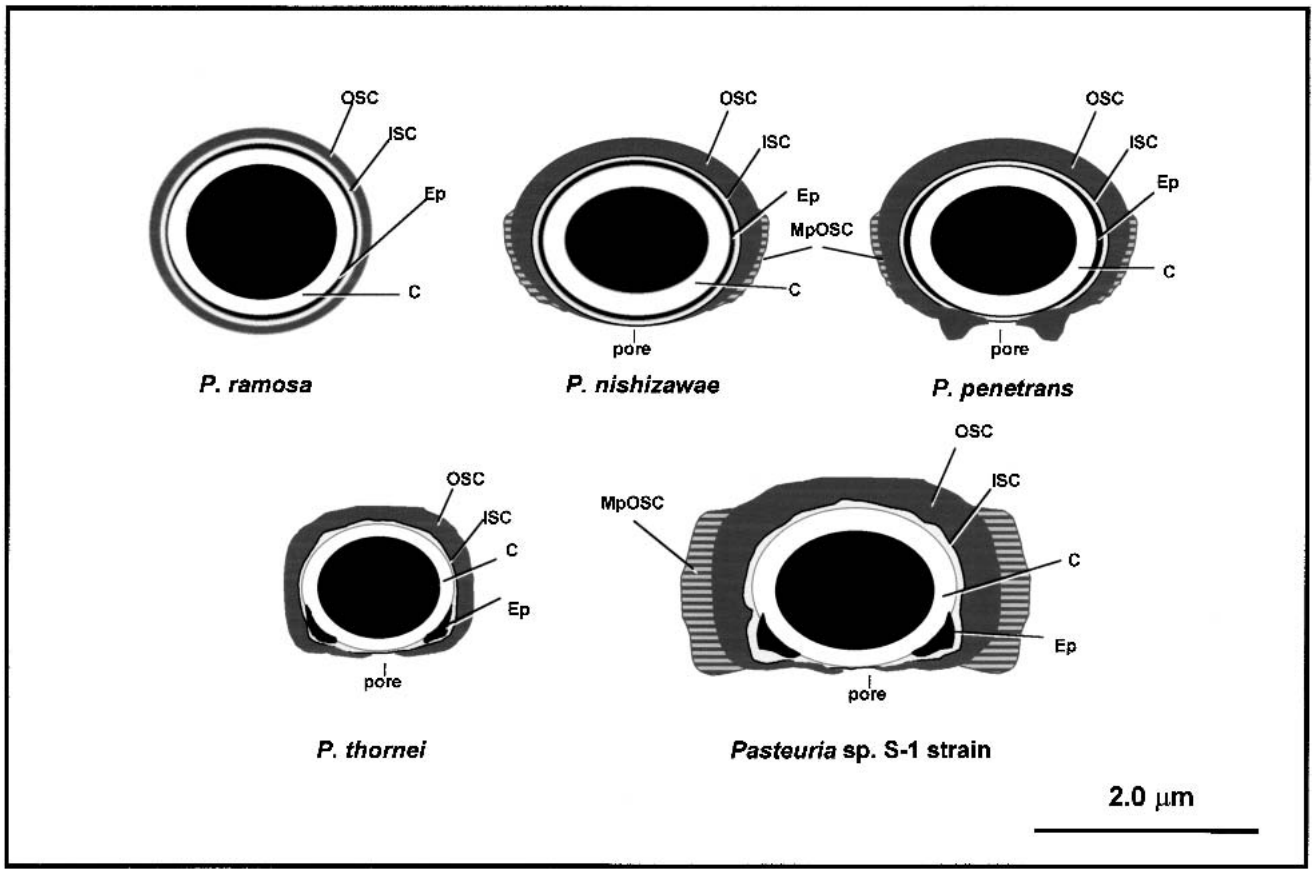

FIG. 5. Diagrammatic drawings depicting the species-diagnostic characters of the central bodies of mature endospores from the four nominal species of *Pasteuria* and S-1 from published TEM photomicrographs or this study (C = cortex; Ep = epicortical wall remnant; ISC = inner spore coat; MpOSC = micro-projections of the outer spore coat; OSC = outer spore coat).

ing lectin ligands on the host nematode cuticle (Brito et al., 1999; Davies and Danks, 1993). The exosporium surfaces of S-1 (Fig. 2), *P. penetrans,* and *P. thornei* are relatively smooth compared with a velutinous surface coat on the exterior surface of the exosporium of *P. nishizawae* (Sayre et al., 1991a, 1991b). Further work is needed to clarify the involvement of the exosporium and sporangium in the attachment process.

Morphometrics of mature endospores of S-1 are presented in Table 1. Cadaver-specific differences existed between the sporangium, central body, and core diameters of S-1 spores, suggesting variation in genetic, nutritional, or developmental parameters (Table 1). When the spore morphometrics from the five cadavers were combined, the measurements were very similar to morphometrics reported previously for this isolate (Giblin-Davis, 2000; Giblin-Davis et al., 1990). The average respective sporangium and central body diameters for S-1 from Davie, Florida, in this study were 6.1 µm (range = 4.9-7.1) and 3.1 (2.4-3.9) (N = 249) (Table 1) compared with 6.1 (4.7-7.0) and 2.9 (2.3-3.8) (N = 418) for S-1-like strains from several locations in southern Florida, including the type site of Davie, Florida (Giblin-Davis et al., 1990).

All stages from second-stage juveniles (J2) through adults of *B. longicaudatus* were observed with attached

TABLE 1. Light microscopic morphometrics (in µm) of mature endospores of S-1 *Pasteuria* sp. from five different *Belonolaimus longicaudatus* cadavers from Davie, FL.

Nematode individual	Mean sporangium diam. (S.D.)*	Mean central body diam. (S.D.)	Mean core diam. (S.D.)	Number of spores
1	6.15A (0.30)	3.18A (0.22)	1.77A (0.23)	49
2	5.99B (0.32)	3.10AB (0.24)	1.51B (0.24)	51
3	6.18A (0.32)	3.10AB (0.25)	1.54B (0.19)	49
4	5.85C (0.42)	3.01B (0.22)	1.42C (0.19)	50
5	6.07AB (0.33)	3.03B (0.23)	1.49BC (0.19)	50
TOTAL	6.05 (0.36) (range=4.92-7.10)	3.08 (0.24) (2.42-3.87)	1.54 (0.24) (1.13-2.26)	249

*S.D. = standard deviation.
Means in a column followed by a different uppercase letter are significantly different ($P \leq 0.05$) according to an LSD multiple range test.

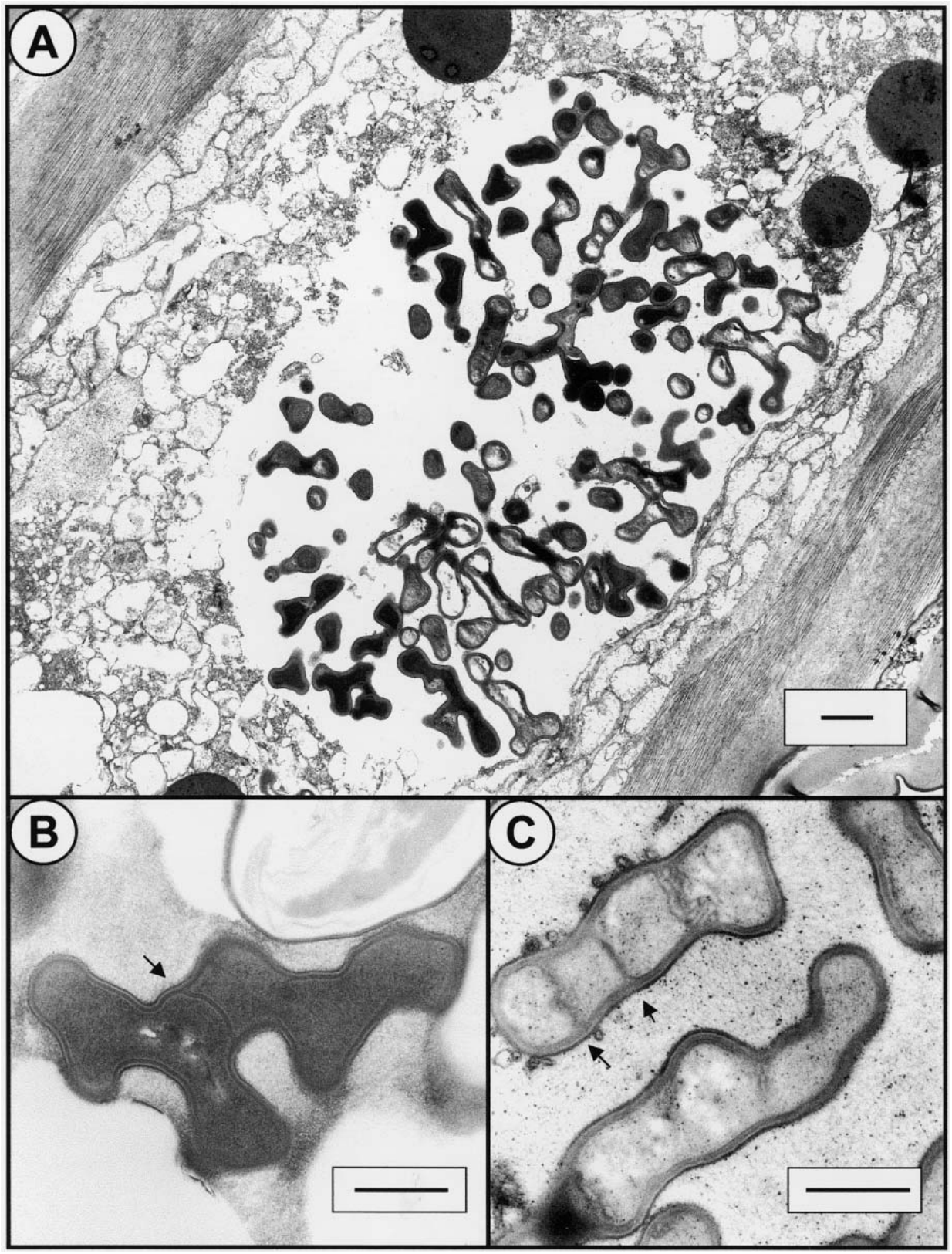

FIG. 6. TEM photomicrographs of *Pasteuria* sp. (S-1 strain) vegetative stage within *Belonolaimus longicaudatus* host showing mycelial growth characteristics. A) Longitudinal section through typical ''cauliflower-like'' mycelial microcolony that is apparently catabolizing hypodermal tissue of the infected host. Bar = 1.0 μm. B) Branching hyphae with septum (arrow). Bar = 0.5 μm. C) Septate (arrows) hyphae with mesosomes. Bar = 0.5 μm.

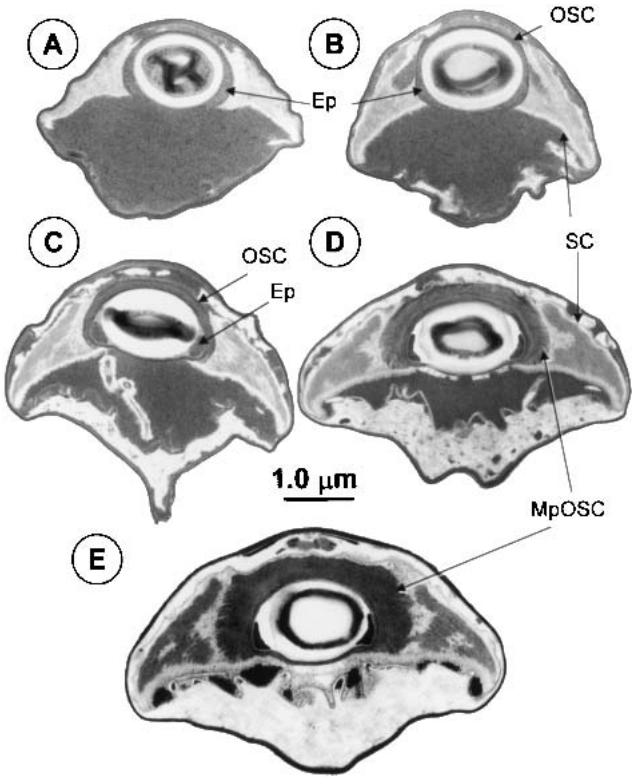

FIG. 7. TEM photomicrographs of stages IV-VII sporogenesis of *Pasteuria* sp. (S-1 strain) in a *Belonolaimus longicaudatus* host (Ep = epicortical wall; MpOSC = microprojections of the outer spore coat; OSC = outer spore coat; SC = surface coat).

endospores of S-1 on the cuticle, and J3 through adults were observed with internal infections of vegetative and sporulating S-1, thus supporting the observations of Bekal et al. (1999). In general, the largest number of attached spores appeared on the head and tail of observed specimens, but spores were observed attached on all body regions, suggesting that cuticular attachment was not restricted to specific areas on *B. longicaudatus* (Fig. 1A, B). The number of attached spores varied from 1 to >200. Attachment studies with J2 of *Meloidogyne incognita, M. javanica, M. arenaria,* and all stages except eggs of *H. galeatus, Pratylenchus penetrans, B. euthychilus,* and *B. longicaudatus* populations from Florida, North Carolina, and Georgia demonstrated that S-1 attaches only to *Belonolaimus* species (Giblin-Davis, 2000; Giblin-Davis et al., 1995). Further attachment studies with S-1 on a wider list of potential hosts, including *Heterodera schachtii, Longidorus africanus, M. hapla, M. incognita, M. javanica, P. brachyurus, P. scribneri, P. neglectus, P. penetrans, P. thornei, P. vulnus,* and *Xiphinema* sp., corroborate these observations (Bekal et al., 2001). These attachment studies are consistent with field work done in southern Florida bermudagrass greens and fairways where S-1 attaches to and completes its life cycle in *B. longicaudatus* alone, even when many other species of nematodes are present in the same sample (e.g., *H. galeatus, Tylenchorhynchus annulatus, Meloidogyne* spp., *Helicotylenchus microlobus, Hemicriconemoides annulatus, Mesocriconema ornata, Trichodorus proximus,* and many free-living nematode species) (Giblin-Davis et al., 1990).

Penetration tubes were observed by light microscopy (LM) issuing from attached spores of S-1 in some specimens. When spores detached after penetration, small remnant ''straws'' could be observed. In some cases, spores that were penetrating during or just prior to the molt could be visualized with a small vesicle-like expansion at its end as observed by Sturhan et al. (1994) for an undescribed species of *Pasteuria* on *Heterodera goettingiana.* With LM, attached spores of S-1 appeared to be viable when they possessed a refractile bulge in the central body as opposed to an empty appearance of a spore devoid of protoplasm (Sturhan et al., 1994). Attached spores stained with acridine-orange and viewed by epifluorescence appeared nacreous when the core was filled with protoplasm and dark when spent.

Previously, TEM observation of nematode penetration has been made only for *P. penetrans* (Sayre and Starr, 1985). We observed the process of penetration for S-1 with TEM (Fig. 4). After attachment, germination appears to begin with the protoplasm becoming granular in appearance (Fig. 4A). A filamentous tube is formed that exits the pore and penetrates the host cuticle (Fig. 4B–D). The penetration tube in the host cuticle is surrounded by a darkened zone, which may result from enzymatic activity (Fig. 4C, D). The penetration tube appeared to penetrate the cortical layer of the cuticle and then traveled parallel to the surface in the porous median zone (Fig. 4C) before penetrating the basal layer of the cuticle, and the muscle (Fig. 4D) into the pseudocoelom. Penetration involved the cortex and protoplasm of the spore as the epicortical wall remnant, inner and outer spore coat, and perisporium were all left behind in germinated spores (Fig. 1E). Scanning electron microscopy examination of an attached spore with the top of the core missing showed that the inner spore coat layer surrounding the pore appears to have pentaradiate symmetry that might function to channel the cortex and protoplasm as they exit the spore and penetrate the host (Fig. 1E). The epicortical wall remnant is also visible in this spent spore (Fig. 1E). The factor(s) responsible for initiation of penetration in S-1 are unknown, although host feeding and molting have been suggested as initiation factors for other species (Sturhan et al., 1994).

Counts of spore-filled cadavers of *B. longicaudatus* showed that juveniles (J3-J4; $n = 5$), males ($n = 5$), and females ($n = 5$) contained averages of 4,700 ± 1,972 (SD) (range = 2,750–7,750), 1,483 ± 1,199 (500–3,500), and 3,633 ± 3,095 (667–7,750) spores/nematode, respectively. Juveniles of *B. longicaudatus* tended to have more spores than adults which, though larger than juveniles, often had areas devoid of spores. *Pasteuria penetrans* and *P. nishizawae* attach to J2 and sporulate only

in mature sedentary females of their respective host species producing 2×10^6 and 4.5×10^5 spores per cadaver, respectively (Sturhan et al., 1994). In comparison, *P. thornei* attaches to and develops in juveniles and adults of *P. brachyurus* producing a few hundred spores per cadaver, and an undescribed species of *Pasteuria* attaches to and develops only in J2 of *H. goettingiana* producing an average of 500 spores per host (Sturhan et al., 1994).

After penetration, a rounded elliptical ''cauliflower-like'' mycelial microcolony is formed, which increases in size in the pseudocoelom (Fig. 6A) similar to what has been reported for other species and strains of *Pasteuria* (Ebert et al., 1996; Sayre et al., 1991b; Starr and Sayre, 1988; Sturhan et al., 1994). With LM, microcolonies of S-1 were most clearly seen in the region of the esophagus. In TEM images, the microcolony appears to cause the dissolution of adjacent tissues (Fig. 6A). Sturhan et al. (1994) report that mycelial colonies are generally found in the pseudocoelom but can also form in the hypodermis or adjacent muscle tissue. Mycelial hyphae are about 0.5 μm in diam., septate, and bounded by an inner and outer wall (Fig. 6B, C). Septa are comprised of constrictions of the inner wall as in other species and strains of *Pasteuria* (Ebert et al., 1996; Starr and Sayre, 1988; Sturhan et al., 1994). Mesosomes (internal membranous structures) were sometimes observed in hyphae (Fig. 6C) and in stages of sporogenesis (Fig. 7C), but this may be a fixation artifact (Chen et al., 1997).

Endospores are produced endogenously, and sporogenesis for S-1 is similar to that in the other species of *Pasteuria* and species of endospore-forming *Bacillus* (Chen et al., 1997; Sturhan et al., 1994). This observation is not surprising because Priest (1993) hypothesized that sporogenesis is highly conserved and probably evolved only once in the bacteria. Stages II-VII of sporogenesis were observed with TEM for S-1 (Figs. 7, 8). Hyphal tips swelled (Fig. 8A) and separated (Fig. 8B). Developing spores were generally not attached to each other or the colony beyond stage II when the forespore septum begins to form (Fig. 8B). Remnant scars from attachment to the mycelial colony are visible (Figs. 7A, C; 8C). During stage III, the sporangium be-

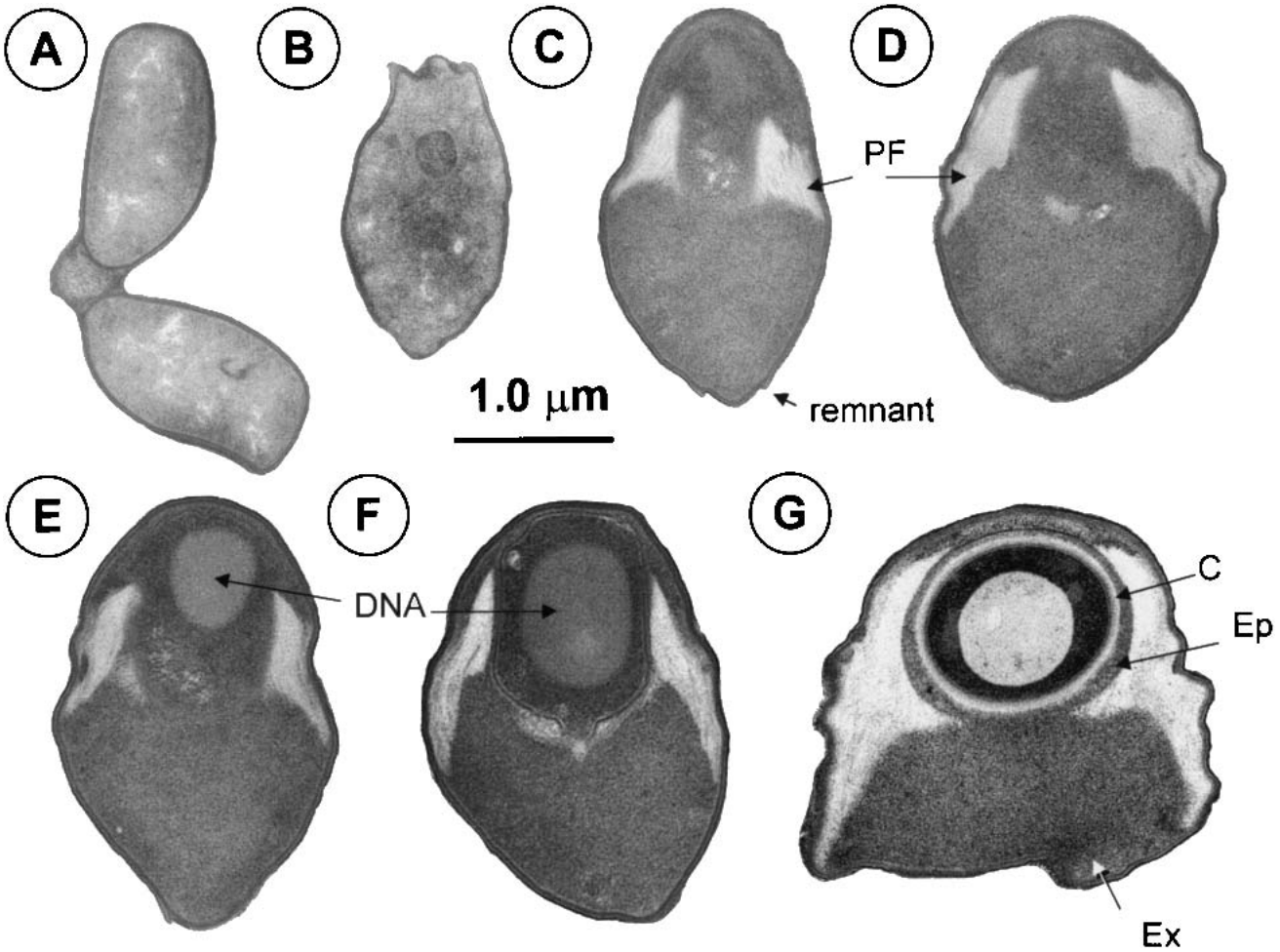

FIG. 8. TEM photomicrographs of early sporogenesis of *Pasteuria* sp. (S-1 strain) in a *Belonolaimus longicaudatus* host. A) Hyphal tip expansion. B) Stage II; beginning formation of forespore septum. C-G) Stage III; formation of the peripheral fibers, inner membrane, cortex, and epicortex (C = cortex; Ep = epicortical wall; Ex = exosporium; PF = peripheral fibers; remnant = scar from attachment to hyphal strand).

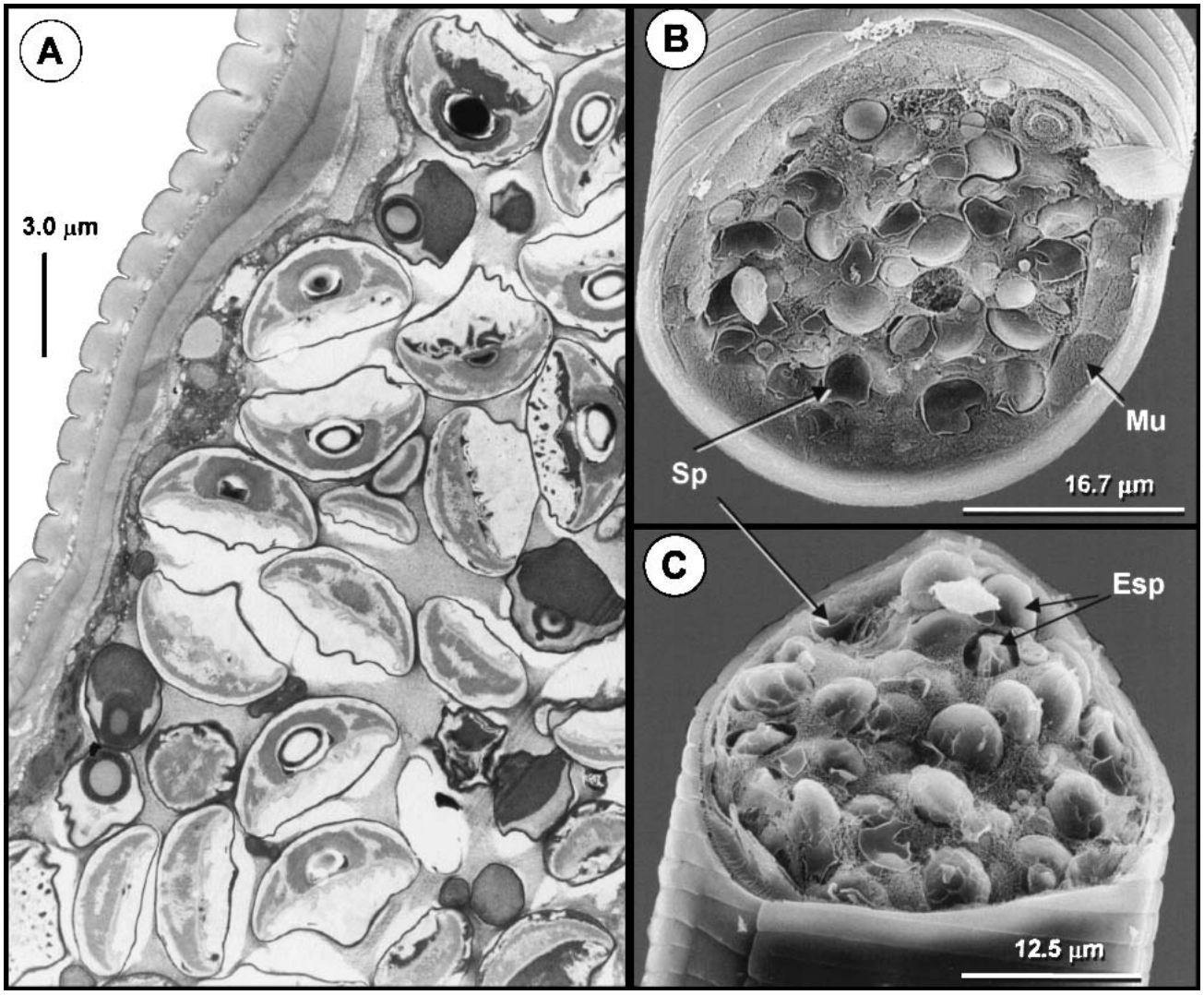

FIG. 9. Sporulation of *Pasteuria* sp. (S-1 strain) in *Belonolaimus longicaudatus* hosts. A) TEM photomicrograph of a longitudinal section showing various stages of sporogenesis. B-C) LTSEM photomicrographs of two different nematode cross-sections showing mostly mature endospores, each within an exosporium and fractured sporangial wall (Esp = endospore; Mu = muscle; Sp = sporangium).

gins to enlarge while maintaining a vertically elongated elliptical shape. The forespore is fully engulfed, and peripheral fibers appear (Fig. 8C-F). A double-layered membrane, which encloses the condensed cytoplasm in the forespore, forms a characteristic apex (future pore) that is directed basally into the cytoplasm of the mother cell (Fig. 8F). A spherical electron-transparent area of the forespore containing DNA becomes visible (Fig. 8E,F). In stage IV, the cortex is formed, the exosporium appears, the peripheral fibers lengthen, and the endospore enlarges laterally (Fig. 8G). In stage V, the endospore continues to enlarge laterally and the spore coats begin to form. Also, a microfibrillar layer begins to appear on the dorsal and ventral surfaces of the peripheral fibers (Fig. 7B, C). The epicortical layer appears surrounding the cortex, thinning on the top and near the pore (Figs. 7A; 8G). The outer spore coat appears dorsally, as a cap that descends around the epicortex and cortex as lamellae and the inner spore coat appears as lamellae that line the outer spore coat (Fig. 7B,C).

As stage V progresses through to VII and concordant with the development of the inner and outer spore coat, the epicortical layer recedes sub-equatorially into a species-characteristic sub-lateral remnant that condenses and becomes more electron opaque as the spore matures (Fig. 7B,C). The amount of granular, electron opaque cytoplasm bounded by the exosporium is depleted as spore maturation proceeds (Fig. 7A–E). Spore maturation continues during stage VII (Fig. 7E). The role of the epicortical layer is unknown but from this study and that of Sturhan et al. (1994) appears to be involved in the development of the early lamellar outer and inner spore coats or perhaps the inner spore coat only. Because the inner spore coat appears solid (Fig. 3B,C), the epicortical wall may become an entrapped remnant of the mother cell cytoplasm that persists into the mature spore. The outer spore coat continues to thicken dorsally and laterally after the inner spore coat has been formed at the same time as the granular, electron opaque cytoplasm between the spore and the exo-

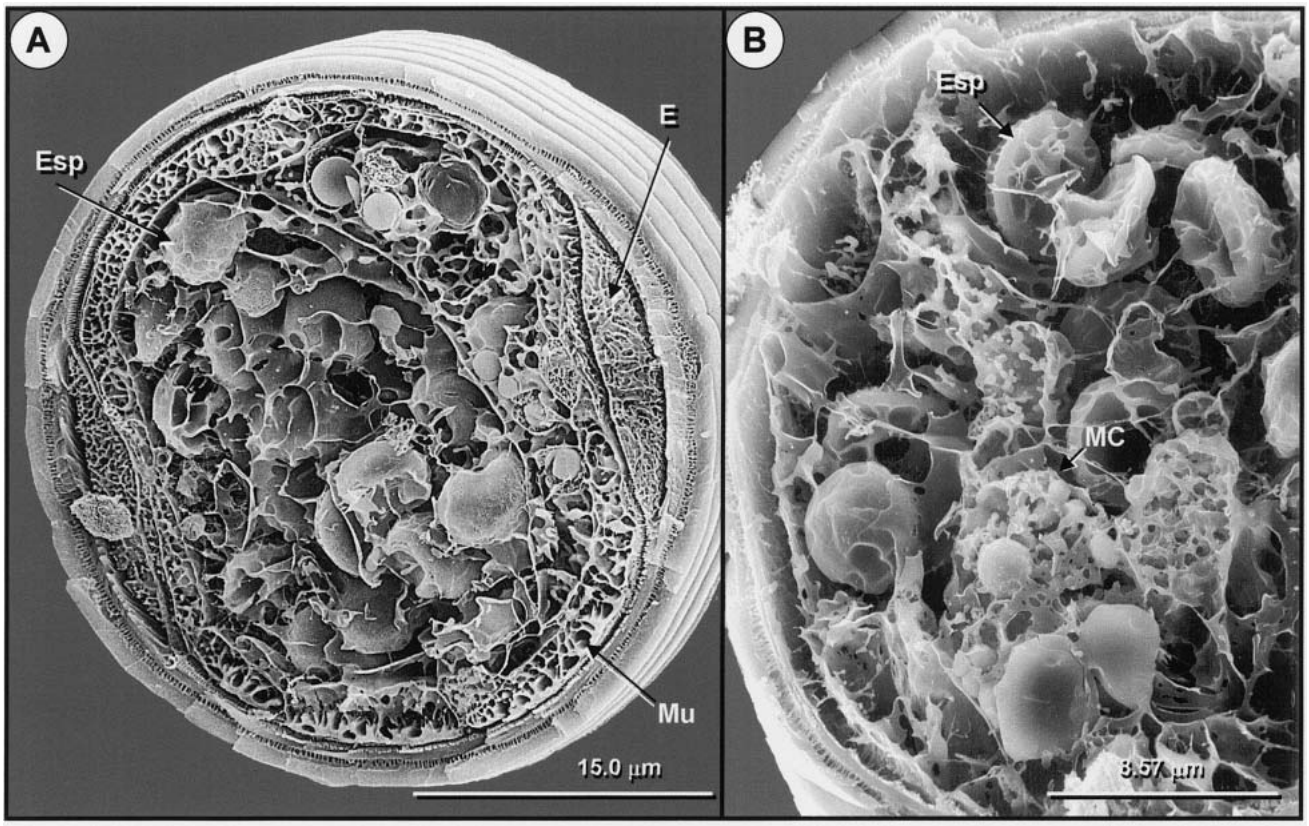

FIG. 10. LTSEM photomicrographs of two different *Belonolaimus longicaudatus* in cross-section and filled with mostly mature endospores of *Pasteuria* sp. (S-1 strain). A) Spores confined to pseudocoelom with evidence of muscle and hypodermal chord catabolism. B) Cross-section near the excretory pore of the host showing mature spores and vegetative stages (Esp = endospore; E = epidermis; MC = mycelial colony; Mu = muscle).

sporium disappears in stages VI and VII (Fig. 7C–E), suggesting that deposition of the outer spore coat is probably accomplished via the perisporium (peripheral fibers and microfibrillar surface coat). Likewise, the microfibrillar surface coat expands as the spore matures, extending the surface area of the perisporium and suggesting a similar ontogeny (Fig. 7E).

As sporogenesis proceeds, the host pseudocoelom fills with spores (Figs. 9, 10). In some sections, the muscles appear unaffected (Fig. 9B). In other sections, the muscles and other tissues appear to be (Fig. 10A) or have been catabolized (Figs. 9A,C; 10B).

Bekal et al. (2001) showed that the 16S rDNA sequence of S-1 (GenBank accession number AF254387) had 96% similarity with previously published *P. penetrans* (Anderson et al., 1999), 93% similarity with *P. ramosa* (Ebert et al., 1996), and 96% similarity with *Pasteuria* sp., isolate NA of *H. glycines* (Atibalentja et al., 2000). A phylogenetic tree constructed by Bekal et al. (2001) showed four main branches within the *Pasteuria* group. Two *P. penetrans* strains cluster together, whereas S-1 is separated from the other three branches with strong bootstrap support (82%). These data support the assertion, based upon a Linnean Species Concept, that S-1 is a unique, undescribed species of *Pasteuria* (Bekal et al., 2001; Giblin-Davis, 2000; Giblin-Davis et al., 1990, 1995). They also provide the foundation for future phylogenetic comparisons of 16S sequences from undescribed *Pasteuria*. Unfortunately, sequence data are not available for two of the described species, *P. thornei* and *P. nishizawae*. The addition of their 16S sequences will be important to the phylogeny and systematics of the group.

LITERATURE CITED

Anderson, J. M., J. F. Preston, D. W. Dickson, T. E. Hewlett, N. H. Williams, and J. E. Muruniak. 1999. Phylogenetic analysis of *Pasteuria penetrans* by 16S rDNA gene cloning and sequencing. Journal of Nematology 31:319–325.

Atibalentja, N., G. R. Noel, and L. L. Domier. 2000. Phylogenetic position of the North American isolate of *Pasteuria* that parasitizes the soybean cyst nematode, *Heterodera glycines,* as inferred from 16S rDNA sequence analysis. International Journal of Systematic and Evolutionary Microbiology 50:605–613.

Bekal, S., J. Borneman, M. S. Springer, R. M. Giblin-Davis, and J. O. Becker. 2001. Phenotypic and molecular analysis of a *Pasteuria* strain parasitic to the sting nematode. Journal of Nematology 33:110–115.

Bekal, S., R. M. Giblin-Davis, and J. O. Becker. 1999. Gnotobiotic culture of *Pasteuria* sp. on *Belonolaimus longicaudatus*. Journal of Nematology 31:522.

Bishop, A. H., and D. J. Ellar. 1991. Attempts to culture *Pasteuria penetrans* in vitro. Biocontrol Science and Technology 1:101–114.

Brito, J. A., J. F. Preston, D. W. Dickson, D. Williams, H. C. Aldrich, R. M. Giblin-Davis, and R. D. Rice. 1999. Immunolocalization of pro-

teins involved in the attachment of *Pasteuria* penetrans to *Meloidogyne arenaria*. Journal of Nematology 31:524.

Chen, Z. X., and D. W. Dickson. 1998. Review of *Pasteuria penetrans*: Biology, ecology, and biological control potential. Journal of Nematology 30:313–340.

Chen, Z. X, D. W. Dickson, L. G. Freitas, and J. F. Preston. 1997. Ultrastructure, morphology, and sporogenesis of *Pasteuria penetrans*. Phytopathology 87:273–283.

Cianco, A. 1995. Phenotypic adaptations in *Pasteuria* spp. nematode parasites. Journal of Nematology 27:328–338.

Cianco, A., R. Bonsignore, N. Vovlas, and F. Lamberti. 1994. Host records and spore morphometrics of *Pasteuria penetrans* group parasites of nematodes. Journal of Invertebrate Pathology 63:260–267.

Cianco, A., V. Vega Farfan, E. Carbonell Torres, and G. Grasso. 1998. Observations on a *Pasteuria* isolate parasitic on *Hoplolaimus galeatus* in Peru. Journal of Nematology 30:206–210.

Davies, K. G., and C. Danks. 1993. Carbohydrate/protein interactions between the cuticle of infective juveniles of *Meloidogyne incognita* and spores of the obligate hyperparasite *Pasteuria penetrans*. Nematologica 39:53–64.

Dickson, D. W., M. Oostendorp, R. M. Giblin-Davis, and D. J. Mitchell. 1994. Control of plant-parasitic nematodes by biological antagonists. Pp. 575–601 *in* D. Rosen, F. D. Bennett, and J. L. Capinera, eds. Pest management in the subtropics. Biological Control—A Florida Perspective. Andover, U.K.:Intercept Ltd.

Ebert, D., P. Rainey, T. M. Embley, and D. Scholz. 1996. Development, life cycle, ultrastructure, and phylogenetic position of *Pasteuria ramosa* Metchnikoff 1888: Rediscovery of an obligate endoparasite of *Daphnia magna* Straus. Philosophical Transactions of the Royal Society of London series B 351:1689–1701.

Giblin-Davis, R. M. 1990. Potential for biological control of phytoparasitic nematodes in bermudagrass turf with isolates of the *Pasteuria penetrans* group. Proceedings of the Florida State Horticultural Society 103:349–351.

Giblin-Davis, R. M. 2000. *Pasteuria* sp. for biological control of the sting nematode, *Belonolaimus longicaudatus,* in turfgrass. Pp. 408–426 in J. M. Clark, and M. P. Kenna, eds. American Chemical Society Symposium Series No. 743: Fate and Management of Turfgrass Chemicals. New York: Oxford Press.

Giblin-Davis, R. M., L. McDaniel, and F. G. Bilz. 1990. Isolates of the *Pasteuria penetrans* group from phytoparasitic nematodes in bermudagrass turf. Journal of Nematology Supplement 22:750–762.

Giblin-Davis, R. M., D. Williams, T. E. Hewlett, and D. W. Dickson. 1995. Development and host attachment studies using *Pasteuria* from *Belonolaimus longicaudatus* from Florida. Journal of Nematology 27: 500.

Jenkins, W. R. 1964. A rapid centrifugal-flotation technique for separating nematodes from the soil. Plant Disease Reporter. 48:692.

Johnson, W. C., and D. J. Tipper. 1981. Acid-soluble spore proteins of *Bacillus subtilis*. Journal of Bacteriology 146:972–982.

Mankau, R. 1975. *Bacillus penetrans* n. comb. causing a virulent disease of plant-parasitic nematodes. Journal of Invertebrate Pathology 26:333–339.

Metchnikoff, M. E. 1888. *Pasteuria ramosa*. Un représentant des bactéries à division longitudinale. Annales de linstitut de Pasteur, Paris 2:165–170.

Priest, F. G. 1993. Systematics and ecology of *Bacillus*. Pp. 3–16 in A. L. Sorenshein, J. A. Hoch, and R. Losick, eds. *Bacillus subtilis* and other gram-positive bacteria: Biochemistry, physiology, and molecular genetics. Washington, D.C.: American Society for Microbiology.

Riese, R. W., K. J. Hackett, R. M. Sayre, and R. N. Huettel. 1988. Factors affecting cultivation of three isolates of *Pasteuria* spp. Journal of Nematology 20:657.

Sayre, R. M., J. R. Adams, and W. P. Wergin. 1979. Bacterial parasite of a cladoceran: Morphology, development in vivo, and taxonomic relationships with *Pasteuria ramosa*. International Journal of Systematic Bacteriology 29:252–262.

Sayre, R. M., R. L. Gherna, and W. P. Wergin. 1983. Morphological and taxonomic re-evaluation of *Pasteuria ramosa* Metchnikoff 1888 and 'Bacillus penetrans' Mankau 1975. International Journal of Systematic Bacteriology 33: 636–649.

Sayre, R. M., and M. P. Starr. 1985. *Pasteuria penetrans* (ex Thorne, 1940) nom. rev., comb. n., sp. n., a mycelial and endospore-forming bacterium parasitic in plant-parasitic nematodes. Journal of the Helminthological Society of Washington 52:149–165.

Sayre, R. M., M. P. Starr, A. M. Golden, W. P. Wergin, and B. Y. Endo. 1988. Comparison of *Pasteuria penetrans* from *Meloidogyne incognita* with a related mycelial and endospore-forming bacterial parasite from *Pratylenchus brachyurus*. Journal of the Helminthological Society of Washington 55:28–49.

Sayre, R. M., W. P. Wergin, T. Nishizawa, and M. P. Starr. 1991a. Light and electron microscopical study of a bacterial parasite from the cyst nematode, *Heterodera glycines*. Journal of the Helminthological Society of Washington 58:69–81.

Sayre, R. M., W. P. Wergin, J. M. Schmidt, and M. P. Starr. 1991b. *Pasteuria nishizawae* sp. nov., a mycelial and endospore-forming bacterium parasitic on cyst nematodes of genera *Heterodera* and *Globodera*. Research in Microbiology 142:551–564.

Starr, M. P. and R. M. Sayre. 1988. *Pasteuria thornei* sp. nov. and *Pasteuria penetrans* senu stricto emend., mycelial and endospore-forming bacteria parasitic, respectively, on plant-parasitic nematodes of the genera *Pratylenchus* and *Meloidogyne*. Annales de linstitut de Pasteur/Microbiology 139:11–31.

Sturhan, D., R. Winkelheide, R. M. Sayre, and W. P. Wergin. 1994. Light and electron microscopical studies of the life cycle and developmental stages of a *Pasteuria* isolate parasitizing the pea cyst nematode, *Heterodera goettingiana*. Fundamental and Applied Nematology 17:29–42.

Wergin, W. P., R. M. Sayre, and E. F. Erbe. 1993. Use of low-temperature scanning electron microscopy to observe frozen hydrated specimens of nematodes. Journal of Nematology 25:214–226.

Williams, A. B., G. R. Stirling, A. C. Hayward, and J. Perry. 1989. Properties and attempted culture of *Pasteuria penetrans*, a bacterial parasite of root-knot nematodes (*Meloidogyne javanica*). Journal of Applied Bacteriology 67:145–156.